

Comparisons of noise spectroscopy analyze and microplasma noise sources

Dolenský J., Vaněk J., Jandová K., Kazelle J., Chobola Z.*

Department of Electrotechnology, Faculty of Electrical Engineering and Communication, Brno University of Technology, Údolní 53, 602 00 Brno, Czech Republic

* Department of Physics, Faculty of Civil Engineering

Brno University of Technology, Žižkova 17, 602 00 Brno, Czech Republic

Abstract

As it was the mechanical noise used for diagnostic of machine in the past, the electronic noise can be used as diagnostic tool for detection defects in electronic devices and systems in the future. This paper deals with comparisons of noise spectroscopy and detection of microplasma noise sources in the three new type of solar cells G1, G3 and G5. When high electric is applied to PN junction with some technological imperfections like dislocation in PN junction or crystal-grid defect causing non-homogeneity of parameters it produces in tiny areas of enhanced impact ionization called microplasma. It can leads onwards to deterioration in quality or to destruction of PN junction. Microplasma produced noise, which has random spectrum in frequency range. Microplasma noise is measurable even before the creation of light emissions. Due to the comparisons microplasma detection with noise characteristic can full analyzed solar cell.

Noise spectroscopy

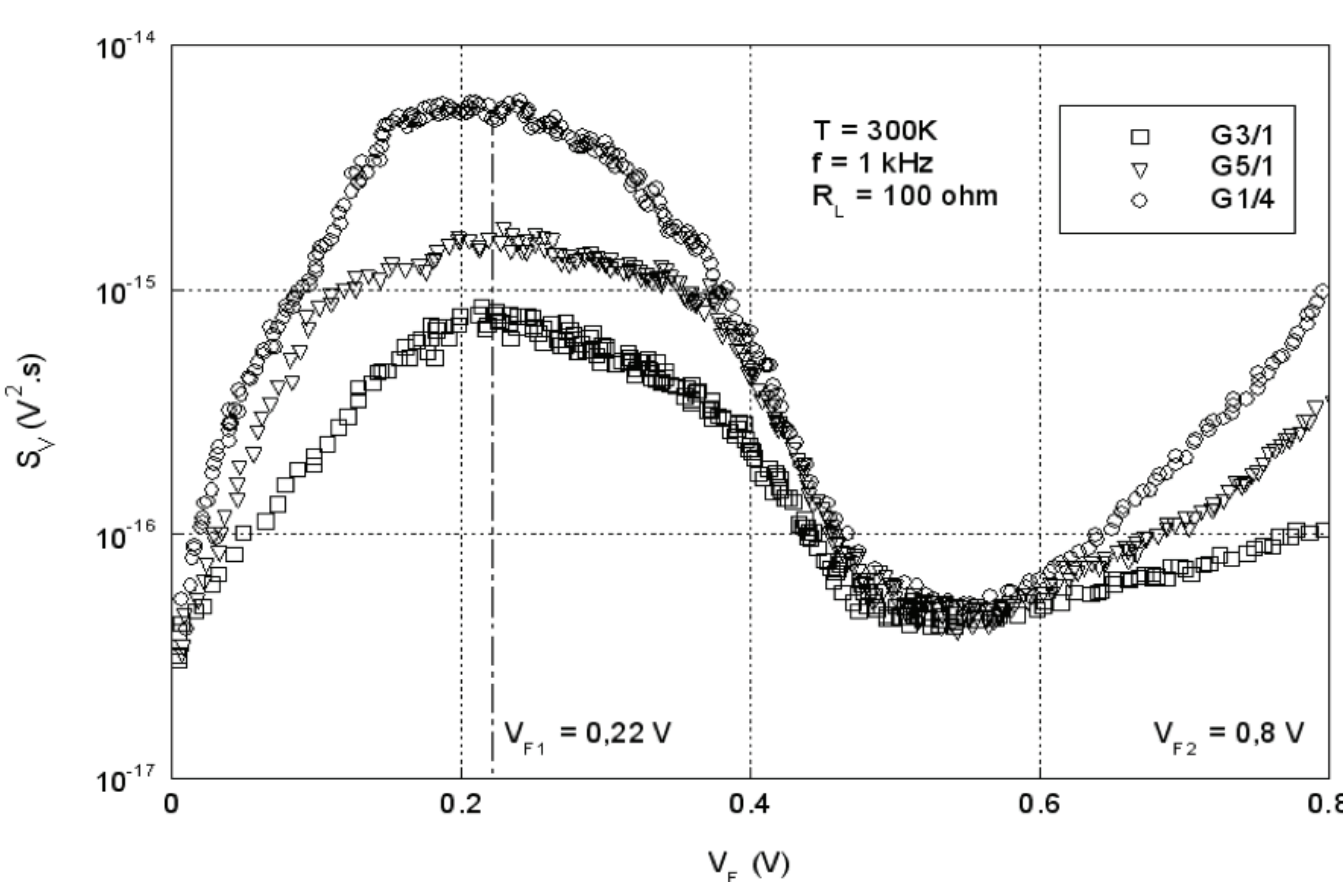


Fig. 1. The noise spectral density as a function of forward voltage for nos. G1/4, G3/1 and G5/1 solar cells in forward direction

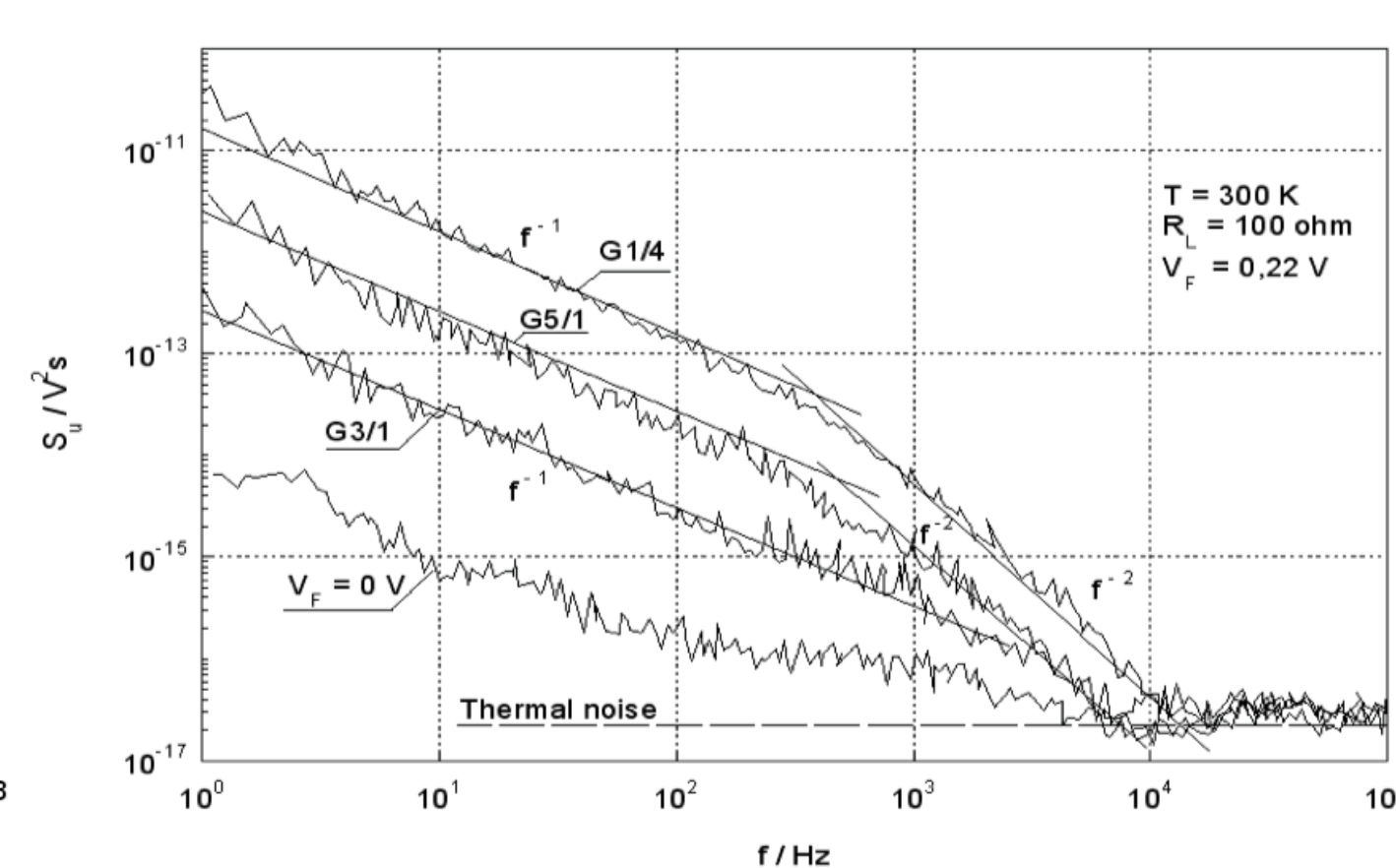


Fig. 2. The noise spectral density versus frequency for mos. for nos. G1/4, G3/1 and G5/1 solar cells in forward direction

Microplasma noise and sources

During increasing reverse biased voltage it is possible to observe more shining points. It was measured with exposure time 20 sec, clear light filter and the CCD chip was cooled into -20°C .

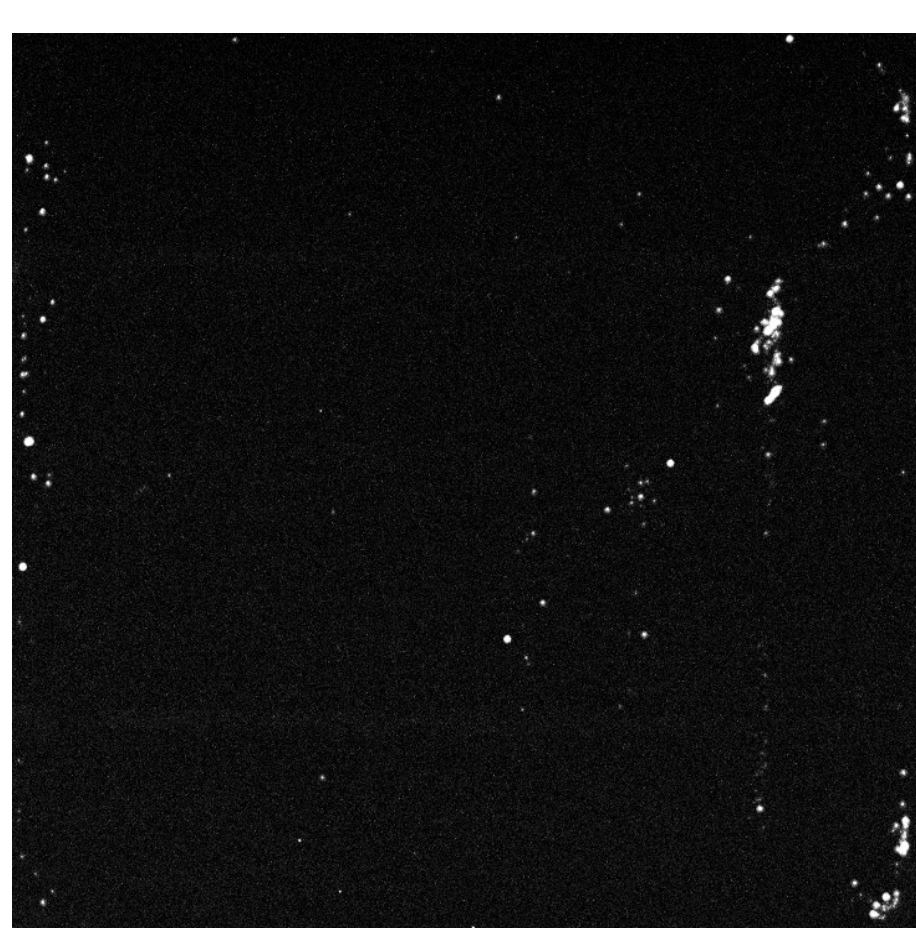


Fig. 3. Cell type G1, $R_{BV} = 4V$, $t_{chip} = -20^{\circ}\text{C}$

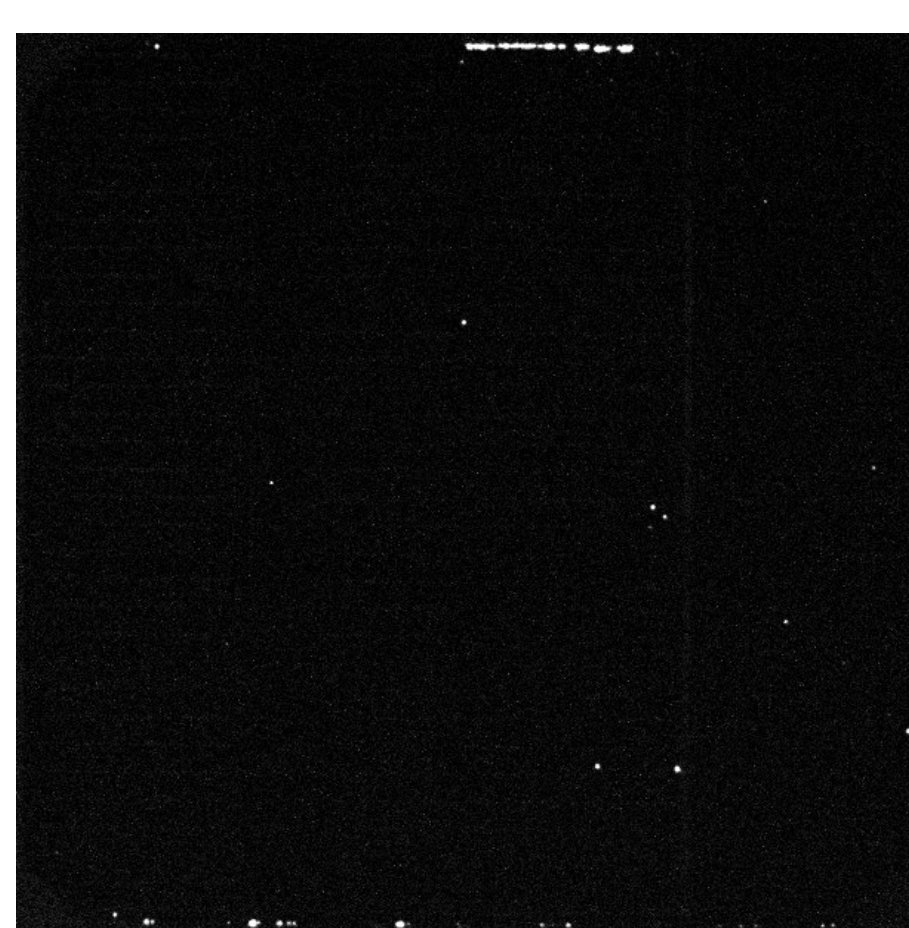


Fig. 4. Cell type G3, $R_{BV} = 4V$, $t_{chip} = -20^{\circ}\text{C}$

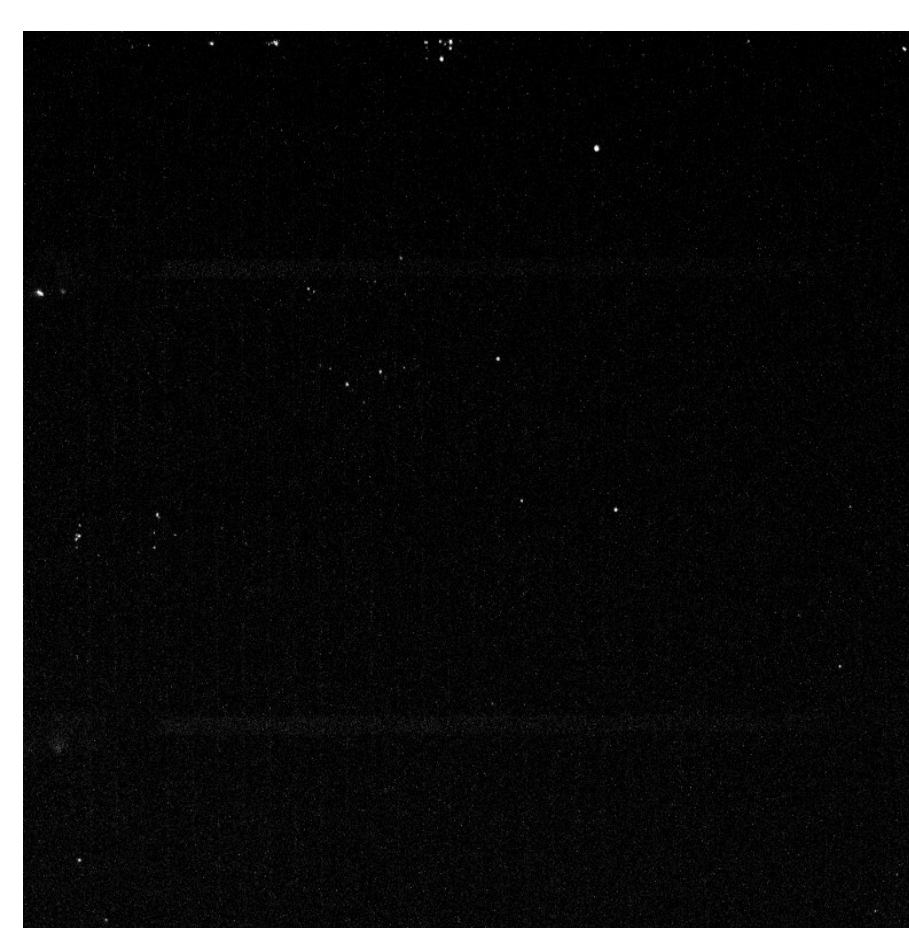


Fig. 5. Cell type G5, $R_{BV} = 4V$, $t_{chip} = -20^{\circ}\text{C}$



Fig. 6. Cell type G1, $R_{BV} = 8V$, $t_{chip} = -20^{\circ}\text{C}$

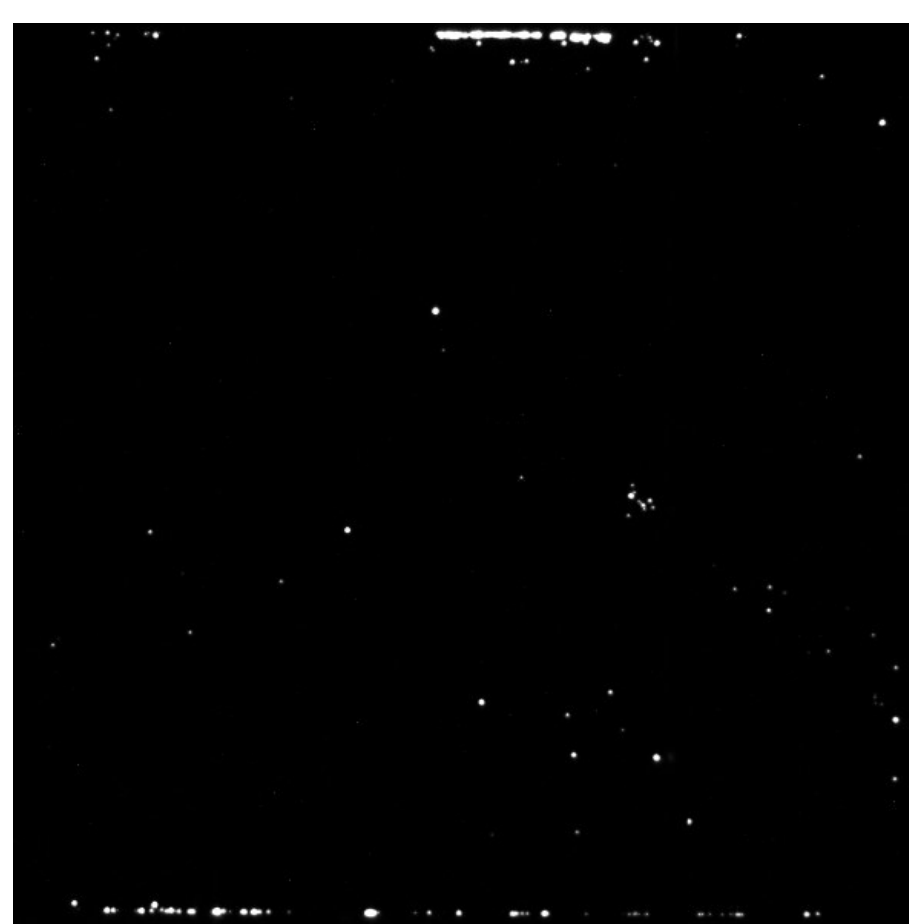


Fig. 7. Cell type G3, $R_{BV} = 8V$, $t_{chip} = -20^{\circ}\text{C}$

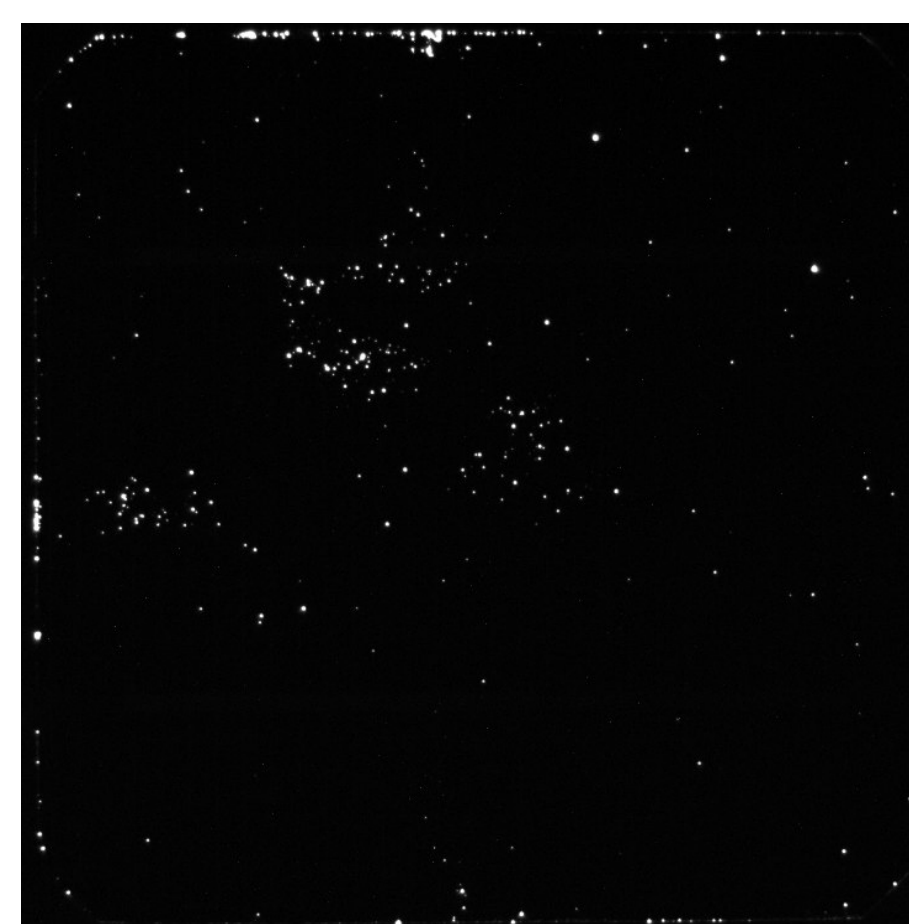


Fig. 8. Cell type G5, $R_{BV} = 8V$, $t_{chip} = -20^{\circ}\text{C}$

Acknowledgements

This work was supported by Ministry of Education (project NO. MSM0021630516).

Specimens

G1 type – this is a standard process. The damaged layer is removed and an alkali-etching-based double-side structuring process is carried out. A double-sided diffusion of an N+ layer follows.

ARC – silicon nitride (Si_3N_4), a variant employing a thin silica layer under the ARC. Finally, thick-film metal plating of both sides is performed.

SPECIMEN	L/A	βV^{-1}	$R_{SH}\Omega$	$R_s\Omega$	$S_{max}V^2s$	$S_{rms}V^2s$
G1/1	$2.5 \cdot 10^{-2}$	18.70	532	0.095	$3 \cdot 10^{-15}$	$8 \cdot 10^{-16}$
G1/4	$3 \cdot 10^{-2}$	18.72	645	0.092	$8 \cdot 10^{-15}$	$1 \cdot 10^{-15}$
G1/5	$7 \cdot 10^{-2}$	18.64	106	0.086	$7 \cdot 10^{-16}$	$7 \cdot 10^{-16}$
G1/7	$8 \cdot 10^{-2}$	18.67	143	0.088	$8 \cdot 10^{-16}$	$7 \cdot 10^{-16}$
σ	$1.7 \cdot 10^{-2}$	18.68	356	0.0902	$3.1 \cdot 10^{-16}$	$8 \cdot 10^{-16}$

Tab. 1. Specimen G1

G3 type – rear side etching process. The damaged layer is removed and an alkali-etching-based double-side structuring process is carried out. A double-sided diffusion of an N+ layer follows. The rear side etching uses an acid solution. ARC – silicon nitride (Si_3N_4) or a variant employing a thin silica layer under the ARC is used. Finally, thick-film metal plating of both sides is performed.

SPECIMEN	L/A	βV^{-1}	$R_{SH}\Omega$	$R_s\Omega$	$S_{max}V^2s$	$S_{rms}V^2s$
G3/1	$8 \cdot 10^{-4}$	19.10	202	0.083	$9 \cdot 10^{-16}$	$1 \cdot 10^{-16}$
G3/3	$7 \cdot 10^{-4}$	19.14	197	0.081	$8 \cdot 10^{-16}$	$1 \cdot 10^{-16}$
G3/5	$7 \cdot 10^{-4}$	19.18	126	0.075	$4 \cdot 10^{-16}$	$9 \cdot 10^{-17}$
G3/7	$1 \cdot 10^{-3}$	19.22	94	0.072	$1.5 \cdot 10^{-16}$	$9 \cdot 10^{-17}$
σ	$8 \cdot 10^{-4}$	19.16	129	0.078	$5.6 \cdot 10^{-16}$	$9.5 \cdot 10^{-17}$

Tab. 2. Specimen G3

G5 type – this is a standard process. The damaged layer is removed and an acid-etching-based double-side structuring process is carried out. A double-sided diffusion of an N+ layer follows.

ARC – silicon nitride (Si_3N_4) or a variant employing a thin silica layer under the ARC is used.

Finally, thick-film metal plating of both sides is performed.

SPECIMEN	L/A	βV^{-1}	$R_{SH}\Omega$	$R_s\Omega$	$S_{max}V^2s$	$S_{rms}V^2s$
G5/1	$1 \cdot 10^{-2}$	18.91	216	0.085	$1.5 \cdot 10^{-15}$	$3 \cdot 10^{-16}$
G5/3	$9 \cdot 10^{-2}$	18.94	203	0.084	$1 \cdot 10^{-15}$	$2 \cdot 10^{-16}$
G5/5	$6 \cdot 10^{-2}$	18.97	98	0.079	$8 \cdot 10^{-16}$	$2 \cdot 10^{-16}$
G5/7	$7 \cdot 10^{-2}$	18.95	132	0.080	$7 \cdot 10^{-16}$	$1 \cdot 10^{-16}$
σ	$8 \cdot 10^{-2}$	18.94	162	0.082	$1 \cdot 10^{-16}$	$2 \cdot 10^{-16}$

Tab. 3. Specimen G5

Conclusion

According to the above described transport and noise characteristic analysis of the mentioned double-sided alkali texture silicon solar cells, it is obvious that better quality has been achieved by the structure of the groups of G3 specimens, this junction (of a thickness of about 1 μm) is etched away from the rear side. The G1 specimens in which an oxide - nitride passivation double layer has been used, show much worse noise properties. The noise parameters are likely to have deteriorated in the course of the high-temperature oxidation as a consequence of additional activation of phosphorus donors in the n+- layer and the subsequent diffusion spreading of the doped layer (which can be recognized from the layer resistance value change). The high thermal stress the Si chips are exposed to can also reduce the minority carrier life time.

SPECIMEN	$R_{BV} = 4V$	$R_{BV} = 8V$
G1	134	181
G3	34	78
G5	30	135

Tab. 4. Counts of microplasma in dependence on reverse biased voltage (R_{BV})

Counts of microplasma highly depends on reversed biased voltage. The results from noise diagnostic shows strong correlation between used texture and noise level. The output from observed microplasma of each cell shows pointed to that the correlation between this two methods can exist. Considering that the correlation is not absolute, counts of microplasma in specimen G5 are not corresponding with noise, further investigation is needed.